

Instruct2Attack: Language-Guided Semantic Adversarial Attacks

Jiang Liu¹, Chen Wei¹, Yuxiang Guo¹, Heng Yu², Alan Yuille¹, Soheil Feizi³,
 Chun Pong Lau⁴✉, Rama Chellappa¹
¹Johns Hopkins University, ²Carnegie Mellon University,
³University of Maryland, College Park, ⁴City University of Hong Kong

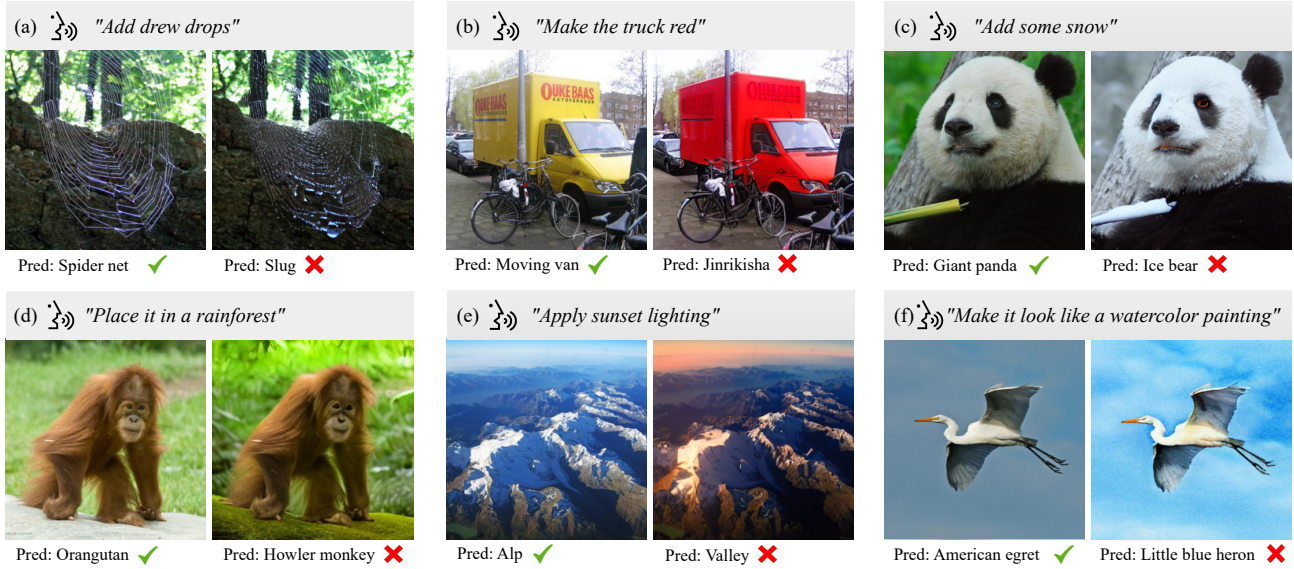


Figure 1. **Examples of Instruct2Attack.** Given an input image (left) and an edit instruction (top banner), our method performs adversarial semantic editing (right) on the original image according to the instruction. The edited images can successfully fool the deep classifier and effectively reveal its vulnerability with subtle semantic changes on, e.g., object shape (a), object color (b), weather (c), background environment (d), lighting condition (e), and image style (f). The edit instructions here are automatically generated by GPT-4.

Abstract

We propose *Instruct2Attack (I2A)*, a language-guided semantic attack that generates semantically meaningful perturbations according to free-form language instructions. We make use of state-of-the-art latent diffusion models, where we adversarially guide the reverse diffusion process to search for an adversarial latent code conditioned on the input image and text instruction. Compared to existing noise-based and semantic attacks, I2A generates more natural and diverse adversarial examples while providing better controllability and interpretability. We further automate the attack process with GPT-4 to generate diverse image-specific text instructions. We show that I2A can successfully break state-of-the-art deep neural networks even under strong adversarial defenses, and demonstrate great transferability among a variety of network architectures.

1. Introduction

Shortly after Deep Neural Networks (DNNs) began to outperform other methods in the field of computer vision [21, 36, 70], their vulnerability with adversarial examples was also discovered [75], which raises crucial security concerns [3]. Specifically, it is demonstrated that DNNs could be fooled by adding small but carefully crafted adversarial noises to the input images, which are imperceptible to human eyes but can cause DNNs to misclassify the images with high confidence.

While earlier work is focused on noise-based attacks [9, 23, 54], recent research explores *semantically meaningful* adversarial examples [32, 61]. Unlike noise-based techniques that produce subtle pixel changes, semantic attacks aim to expose systemic vulnerabilities through semantic manipulations. For instance, an image classifier could

be fooled by adversarial semantic image editing that is not supposed to change the object category, such as spatial [17, 19, 81] and color transforms [29, 37, 89], global style transformation [33, 69], attribute editing [32, 61] and other semantic perturbations [46, 82]. Such adversarial examples provide additional insights into model failure modes beyond pixel-wise perturbations and address criticisms that noise-based attacks lack interpretability and naturalness, and fail to capture model failures in the real world.

A key challenge in crafting semantic adversarial examples is making controlled edits that only change a specific attribute while preserving other semantics. Previous approaches [61, 69] have applied generative adversarial networks (GANs) for controllable image editing [22, 62, 92]. However, GANs have limited disentanglement capabilities for complex real-world images beyond structured face and street-view images. It is also not easy for GAN-based image editing to arbitrarily manipulate any semantics, such as through natural language instructions. Recent advances in controllable image generation and editing with diffusion models [28, 55, 72] have opened new opportunities for designing semantic adversarial attacks. For instance, Instruct-Pix2Pix [8] enables text-driven image manipulation by conditioning on an input image and a written instruction to produce an edited result. This approach demonstrates impressive capabilities in following free-form language instructions to make targeted changes to diverse images.

Building on recent advances in controllable image editing, we propose Instruct2Attack (I2A), a novel attack method that generates realistic and interpretable semantic adversarial examples guided by free-form language instructions. Specifically, our approach leverages a latent conditional diffusion model [8, 66] which has two conditions: One is the input image to perturb, and the other is the language instruction defining semantic attributes to modify. Controlled by two learnable adversarial guidance factors corresponding to the image and text guidance respectively, I2A navigates in the latent space to find an adversarial latent code that generates semantic adversarial images for the targeted victim models. The generated adversarial examples selectively edit attributes based on the language instruction while preserving unrelated image context. Additionally, we impose a perceptual constraint to ensure the similarity between the input image and the adversarial image.

Our method reveals the vulnerability of the victim models in various situations with a simple control knob of natural languages. We further explore automating the process with GPT-4 [59] to generate diverse and image-specific text instruction as illustrated in Fig. 1. The proposed I2A attack introduces natural and diverse semantic perturbations based on text instructions. Quantitative experiments demonstrate that I2A delivers high attack success rates, especially under strong adversarial training-based [18, 45, 68, 71, 80]

and preprocessing-based [57] defenses, where I2A consistently outperforms previous adversarial attack methods by a large margin. For example, I2A can effectively break the strongest Swin-L [45, 50] model on the Robustbench [13] ImageNet leaderboard, bringing down the robust accuracy from 59.56% to 4.98%. Moreover, we demonstrate that I2A achieves great attack transferability among a variety of model architectures under the black-box setting.

2. Related Work

L_p and non- L_p attack. L_p attack [9, 23, 40, 47, 48, 54] optimizes adversarial noises within a small L_p ball, which is the most popular form of adversarial attacks. L_p adversarial samples are often imperceptible but they are shown to have a distribution gap from the natural images [84]. On the other hand, non- L_p attack generalizes L_p attack by using non- L_p metrics to bound the perturbations [33, 38, 89] or even generating unbounded perturbations [7], which allows large and perceptible perturbations.

Semantic attack. Semantic attack is a type of non- L_p attack that aims to alter the semantic content or context of the input. Semantic attack creates interpretable perturbations that are more relevant in real-world scenarios. Early works in semantic attacks are limited to simple transformations including spatial transform [17, 19, 81], color transforms [29, 37, 89], and brightness adjustment [82]. More recent work includes global style transformation [33, 69], and fixed-category attribute editing [32, 61]. Compared to existing works, I2A is capable of generating more sophisticated and flexible semantic manipulations based on free-form language instructions.

Latent space attack. Instead of adding perturbations in the image space, latent space attacks perturb the latent representation of the input image, which is usually in the latent space of generative models, such as GANs [31, 39, 43], flow-based models [41, 87] and diffusion models [11, 49, 79, 83]. Latent space attacks generate more structured perturbations than image space attacks. However, these perturbations usually lack semantic meaning and are hard to interpret.

Image editing using generative models. Image editing [44, 52, 53, 58] denotes the process of manipulating a given image by certain semantic attributes, such as style transfer and image domain translation. It requires the techniques from semantic image synthesis [30, 60, 76] and image inpainting [85, 86, 89]. Various editing approaches first encode [10, 65] or invert [1, 2, 4] images to obtain the corresponding latent representation and edit the images by manipulating the latent vectors. Recently, text encoders such as CLIP [63] or BERT [34] are also employed to guide the image editing process with text using GAN models [14, 14, 20] or diffusion models [6, 8, 25, 35, 56].

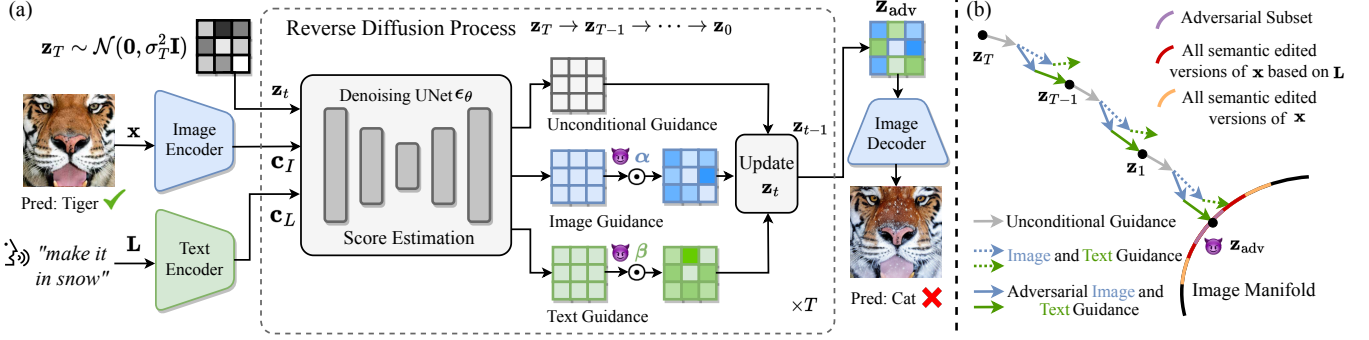


Figure 2. (a) **Overview of the Instruct2Attack (I2A) framework.** (b) **Illustration of adversarial diffusion guidance.** Given the input image and text instruction as conditions, I2A adversarially guides the reverse diffusion process to search for an adversarial code in the latent space by modulating the image and text guidance with the adversarial guidance factors α and β .

3. Method

3.1. Problem Definition

In this paper, we consider the task of image classification. Suppose an image sample $\mathbf{x} \in \mathcal{X} := \mathbb{R}^{H \times W \times C}$ and its corresponding label $y \in \mathcal{Y} := \{1, \dots, |\mathcal{Y}|\}$ are drawn from an underlying distribution $\mathbb{P} := \mathcal{X} \times \mathcal{Y}$, where H , W and C are the height, width and the number of channels of the image, respectively. Let $f: \mathcal{X} \rightarrow \mathcal{Y}$ be an image classifier. Given a clean input image \mathbf{x} and the corresponding ground-truth label y , the goal of the attacker is to craft an adversarial image \mathbf{x}_{adv} of \mathbf{x} to fool f , such that $f(\mathbf{x}_{adv}) \neq y$.

A popular way to construct \mathbf{x}_{adv} is by adding pixel-wise adversarial noise δ [9, 23, 54] to the input image \mathbf{x} , i.e., $\mathbf{x}_{adv} = \mathbf{x} + \delta$. Although it has been shown that noise-based attacks are successful in breaking DNNs, δ lacks semantic meanings and is unlikely to exist in natural images, which makes it hard to interpret why they cause the failures of DNNs. In this work, we instead consider language-guided semantic attacks, where we aim to generate semantically meaningful perturbations guided by free-form languages. These natural and interpretable perturbations provide valuable insights into understanding the failure modes of DNNs.

3.2. Instruct2Attack (I2A)

Our method aims to solve for \mathbf{x}_{adv} that lies on the natural image manifold, where the difference between \mathbf{x} and \mathbf{x}_{adv} is controlled by an edit instruction \mathbf{L} . To achieve this, we make use of the learned latent space of a generative model $\mathcal{Z} = \{\mathbf{z} \mid \mathbf{z} = \mathcal{E}(\mathbf{x}), \mathbf{x} \in \mathcal{X}\} \subseteq \mathbb{R}^{h \times w \times c}$, where \mathcal{E} is the image encoder, and $h \times w \times c$ is the dimension of the latent space. Compared to image space, the latent space provides a low-dimensional compact representation that focuses on the important, semantic information of the data, which is more suitable for semantic editing. We then aim to search for an adversarial latent code \mathbf{z}_{adv} according to the conditional distribution $p(\mathbf{z}|\mathbf{x}, \mathbf{L})$, which can be modeled by a pretrained conditional latent diffusion model (LDM) [8, 66].

Overview. The overview of I2A is in Fig. 2 (a). We start with a random noise $\mathbf{z}_T \sim \mathcal{N}(\mathbf{0}, \sigma_T^2 \mathbf{I})$ in the latent space,

where σ_T is the noise scale. We then iteratively refine \mathbf{z}_T in the reverse diffusion process using a denoising U-Net [67] ϵ_θ with the input image \mathbf{x} and text instruction \mathbf{L} as conditions to move it towards $p(\mathbf{z}|\mathbf{x}, \mathbf{L})$. At each denoising step, we adversarially guide the diffusion process to reach an adversarial latent code \mathbf{z}_{adv} , which is controlled by the learnable adversarial guidance factors α and β that are obtained by optimizing Eq. (6). The final output is reconstructed by the image decoder \mathcal{D} , i.e., $\mathbf{x}_{adv} = \mathcal{D}(\mathbf{z}_{adv})$.

Image and text conditioning. The reverse diffusion process is conditioned on the input image \mathbf{x} and the edit instruction \mathbf{L} . This is implemented with a conditional denoising U-Net $\epsilon_\theta(\mathbf{z}_t, \mathbf{c}_I, \mathbf{c}_L)$. Specifically, \mathbf{x} is first encoded by the image encoder \mathcal{E} to obtain the image condition embedding $\mathbf{c}_I = \mathcal{E}(\mathbf{x}) \in \mathbb{R}^{h \times w \times c}$ and \mathbf{L} is encoded by a text encoder \mathcal{C} to obtain the text condition embedding $\mathbf{c}_L = \mathcal{C}(\mathbf{L}) \in \mathbb{R}^{m \times l}$. At each denoising step, \mathbf{c}_I is concatenated with \mathbf{z}_t as the input to ϵ_θ , while \mathbf{c}_L is projected to the intermediate layers of ϵ_θ via a cross-attention layer [78].

Adversarial diffusion guidance. Let \mathbf{z}_0 be the denoised output of \mathbf{z}_T through the reverse diffusion process $\mathbf{z}_0 := \text{LDM}(\mathbf{z}_T; \mathbf{c}_I, \mathbf{c}_L)$. In a benign editing setting, \mathbf{z}_0 is computed by the following iterative denoising equation [73]:

$$\mathbf{z}_{t-1} = \mathbf{z}_t + (\sigma_t^2 - \sigma_{t-1}^2)e_\theta(\mathbf{z}_t, \mathbf{c}_I, \mathbf{c}_L) + \sqrt{\frac{\sigma_{t-1}^2(\sigma_t^2 - \sigma_{t-1}^2)}{\sigma_t^2}}\boldsymbol{\zeta}_t, \quad (1)$$

where $1 \leq t \leq T$ is the time step, σ_t is the noise scale, $\boldsymbol{\zeta}_t \sim \mathcal{N}(\mathbf{0}, \mathbf{I})$. e_θ is the modified score estimate [66] based on classifier-free guidance [27] to improve sample quality:

$$\begin{aligned} e_\theta(\mathbf{z}_t, \mathbf{c}_I, \mathbf{c}_L) &= e_\theta(\mathbf{z}_t, \emptyset_I, \emptyset_L) \\ &\quad + s_I \cdot (e_\theta(\mathbf{z}_t, \mathbf{c}_I, \emptyset_L) - e_\theta(\mathbf{z}_t, \emptyset_I, \emptyset_L)) \\ &\quad + s_T \cdot (e_\theta(\mathbf{z}_t, \mathbf{c}_I, \mathbf{c}_L) - e_\theta(\mathbf{z}_t, \mathbf{c}_I, \emptyset_L)), \end{aligned} \quad (2)$$

where the first term is the unconditional guidance, the second term is the image guidance, the third term is the text guidance, \emptyset_I and \emptyset_L are the fixed null values for image and text conditionings respectively, and s_I and s_T are the image

Algorithm 1 Instruct2Attack

```

1: Input:  $\mathbf{x}, \mathbf{T}, y, \gamma, \eta, \lambda, T, s_I, s_T, N, f, \epsilon_\theta, \mathcal{E}, \mathcal{D}, \mathcal{C}$ 
2: Output: adversarial image  $\mathbf{x}_{\text{adv}}$ 
3:  $\triangleright$  Initialize the latent code
4:  $\mathbf{z}_T \sim \mathcal{N}(\mathbf{0}, \sigma_T^2 \mathbf{I})$ 
5:  $\triangleright$  Image and text encoding
6:  $\mathbf{c}_I = \mathcal{E}(\mathbf{x}), \mathbf{c}_L = \mathcal{C}(\mathbf{L})$ 
7:  $\triangleright$  Optimize  $\alpha$  and  $\beta$ 
8:  $\alpha \leftarrow \vec{1}, \beta \leftarrow \vec{1}$ 
9: for  $i = 0$  to  $N - 1$ 
10:  $\mathbf{z}_{\text{adv}} = \text{LDM}(\mathbf{z}_T; \mathbf{c}_I, \mathbf{c}_L, \alpha, \beta)$   $\triangleright$  Sample  $\mathbf{z}_{\text{adv}}$ 
11:  $\mathbf{x}_{\text{adv}} = \mathcal{D}(\mathbf{z}_{\text{adv}})$   $\triangleright$  Generate  $\mathbf{x}_{\text{adv}}$ 
12:  $\mathcal{L} = \mathcal{L}_c(\mathbf{x}_{\text{adv}}, y) - \lambda \max(0, d(\mathbf{x}_{\text{adv}}, \mathbf{x}) - \gamma)$ 
13: Update  $\alpha$  and  $\beta$  according to Eq. (7)
14: if  $f(\mathbf{x}_{\text{adv}}) \neq y$  and  $d(\mathbf{x}_{\text{adv}}, \mathbf{x}) \leq \gamma$   $\triangleright$  Early stopping
15:   break
16: end if
17: end for

```

and text guidance scales. To adversarially guide the diffusion process to find an adversarial latent code \mathbf{z}_{adv} , we introduce two adversarial guidance factors $\alpha, \beta \in [0, 1]^{h \times w \times c}$ that adversarially modulate the image guidance and text guidance at each diffusion step, as illustrated in Fig. 2 (b):

$$\begin{aligned}
\tilde{\epsilon}_\theta(\mathbf{z}_t, \mathbf{c}_I, \mathbf{c}_L) = & \epsilon_\theta(\mathbf{z}_t, \emptyset_I, \emptyset_L) \\
& + s_I \cdot \alpha \odot (\epsilon_\theta(\mathbf{z}_t, \mathbf{c}_I, \emptyset_L) - \epsilon_\theta(\mathbf{z}_t, \emptyset_I, \emptyset_L)) \\
& + s_T \cdot \beta \odot (\epsilon_\theta(\mathbf{z}_t, \mathbf{c}_I, \mathbf{c}_L) - \epsilon_\theta(\mathbf{z}_t, \mathbf{c}_I, \emptyset_L)),
\end{aligned} \quad (3)$$

where \odot is the Hadamard product. Note that α and β are not scalars but vectors, which provides more flexibility in controlling the diffusion process.

Perceptual constraint. To preserve the similarity between \mathbf{x} and \mathbf{x}_{adv} while allowing for semantic editing, we propose to use the perceptual similarity metric LPIPS [38, 88] instead of the typical pixel-wise L_p distance to bound the adversarial perturbation. The LPIPS distance between two images \mathbf{x}_1 and \mathbf{x}_2 is defined as:

$$d(\mathbf{x}_1, \mathbf{x}_2) \triangleq \|\phi(\mathbf{x}_1) - \phi(\mathbf{x}_2)\|_2, \quad (4)$$

where $\phi(\cdot)$ is a feature extraction network. Formally, we aim to solve the following optimization problem:

$$\max_{\alpha, \beta} \mathcal{L}_c(\mathbf{x}_{\text{adv}}, y), \text{ s.t., } d(\mathbf{x}_{\text{adv}}, \mathbf{x}) \leq \gamma, \quad (5)$$

where $\mathbf{x}_{\text{adv}} = \mathcal{D}(\mathbf{z}_{\text{adv}}) = \mathcal{D}(\text{LDM}(\mathbf{z}_T; \mathbf{x}, \mathbf{L}, \alpha, \beta))$, γ is the perturbation budget, and \mathcal{L}_c is the cross-entropy loss. In practice, it is hard to solve Eq. (5) directly given the LPIPS constraint and we use a Lagrangian relaxation of Eq. (5):

$$\max_{\alpha, \beta} \mathcal{L} = \mathcal{L}_c(\mathbf{x}_{\text{adv}}, y) - \lambda \max(0, d(\mathbf{x}_{\text{adv}}, \mathbf{x}) - \gamma), \quad (6)$$



BLIP-2 “a panda bear is looking at the camera” “a baby’s crib with a blue canopy and a white net” “two white dogs sitting in a yellow tub”

GPT-4 “Add bamboo in background.” “Add a teddy bear.” “Fill the tub with water.”

Figure 3. **Examples of automatic instruction generation.** We first use BLIP-2 [42] to generate image captions and feed them into GPT-4 [59] to generate image-specific semantic edit instructions.

where λ is the Lagrange multiplier. The second term in Eq. (6) grows linearly with $d(\mathbf{x}_{\text{adv}}, \mathbf{x})$ when it is greater than γ and becomes 0 when the perceptual constraint $d(\mathbf{x}_{\text{adv}}, \mathbf{x}) \leq \gamma$ is satisfied. We iteratively solve Eq. (6) with projected gradient descent:

$$\begin{cases} \alpha^{(i+1)} = \mathcal{P}(\alpha^{(i)} + \eta \cdot \text{sign} \nabla_{\alpha^{(i)}} \mathcal{L}), \\ \beta^{(i+1)} = \mathcal{P}(\beta^{(i)} + \eta \cdot \text{sign} \nabla_{\beta^{(i)}} \mathcal{L}), \end{cases} \quad (7)$$

where \mathcal{P} is the projection onto $[0, 1]^{h \times w \times c}$, $0 \leq i < N$ is the attack step, N is the maximum attack iteration, η is the step size, and α and β are initialized as all-one vectors $\vec{1}$. The I2A algorithm is summarized in Algorithm 1. At the end of the attack generation, we ensure the perceptual constraint is satisfied by projecting \mathbf{x}_{adv} back to the feasible set through dynamically adjusting s_I and s_T in Eq. (3) which control the trade-off between how strongly the edited image corresponds with the input image and the edit instruction. The details of the projection algorithm are in the Supp.

3.3. Automatic Instruction Generation

An important component of I2A is the input text instruction. While the text instructions can be any user-defined prompts, they should be legitimate to produce natural and plausible semantic modifications without alternating object categories. Ideally, the text instruction should be determined based on the image context. However, it is infeasible to manually write such image-specific prompts for every image in a large dataset. To address this challenge, we leverage large vision and language models to automatically generate image-specific editing instructions. We first convert the input image to an image caption using BLIP-2 [42]. Then we apply the language-only GPT-4 [59] to generate editing instructions based on the input captions and object categories. We utilize few-shot in-context learning by presenting 50 manually written examples in the prompt without fine-tuning the GPT-4 model. GPT-4 is instructed to “generate natural and simple image editing instructions without

altering the inherent nature or category of objects within the image". The full prompt for GPT-4 can be found in the supplementary material. Examples of automatically generated image captions and edit instructions are shown in Fig. 3. The proposed method can generate relevant image editing instructions based on the image content.

4. Experiments and Results

4.1. Settings

Datasets and metrics. We evaluate I2A on the ImageNet [15] subset used by Robustbench [13], which consists of 5,000 randomly sampled images from the ImageNet validation set. We additionally evaluate I2A on Places365 [91], a scene recognition dataset with 365 scene classes. We randomly selected ten images for each class from the validation set, resulting in a subset of 3,650 images. All images are resized to $256 \times 256 \times 3$. We adopt top-1 classification accuracy to evaluate the attack effectiveness.

Implementation details. We use four manually written editing instructions and the instructions generated by GPT4 for evaluation, resulting in five editing prompts per image. Unless mentioned otherwise, we report the average accuracy of the five edit prompts for I2A. The manually written instructions include instructions that change the lighting ("make it at night"), weather conditions ("make it in snow"), and overall image styles ("make it a sketch painting", "make it a vintage photo"). These are general edits applicable to every image. We set $\lambda = 100$, $\gamma = 0.3$, $\eta = 0.1$, $T = 20$, $s_I = 1.5$, $s_T = 7.5$, and $N = 200$. The latent space dimension is $32 \times 32 \times 4$. We use the pretrained AlexNet [36] as the feature network ϕ for LPIPS. For \mathcal{E} , \mathcal{D} , \mathcal{C} and ϵ_θ , we use the pretrained weights of [8] and keep the weights frozen during attack generation. More details are in the Supp.

4.2. Results on ImageNet

Baselines. We consider L_p attacks including FGSM [23], PGD [54], MIM [16] and AutoAttack [12], and non- L_p attacks including Fog, Gabor, Elastic, Snow [33], StAdv [81] and PerC-AL [90] for comparisons. For L_p attacks, we use L_∞ norm with a bound of $4/255$. The implementation details of the baselines can be found in the Supp.

Victim models. We consider a variety of networks, from convolutional ResNet-18/50 [24] and the recent ConvNeXt-B/L [51], to Transformer-based Swin-B/L [50].

Defense methods. To better understand the attack performance under defenses, we evaluate both *undefended* and *defended* models for each network architecture. We consider adversarial training-based defenses, including models trained by Salman2020 [68], Engstrom2019 [18], Fast AT [80], ARES-Bench [45], and ConvStem [71], which

are top-performing models on the Robustbench ImageNet leaderboard [13]. We also evaluate the attack methods on a state-of-the-art preprocessing-based defense DiffPure [57], which aims to remove adversarial perturbations using a diffusion model. Details of defense methods are in the Supp.

White-box attack. We compare I2A with baseline attacks under the white-box attack setting in Table 1. Overall, I2A achieves the lowest average classification accuracy, which is significantly lower than the second best method StAdv [81] (16.90% vs. 37.81%). In addition, we find that I2A is highly effective for adversarially trained models. In particular, Swin-L trained by ARES [45] is the current strongest model on the Robustbench ImageNet leaderboard [13], which achieves 59.56% accuracy under AutoAttack [12] but only 4.98% under the proposed I2A attack. These results suggest that I2A reveals new vulnerabilities in DNNs. Another interesting finding from Table 1 is that undefended models are slightly more robust to the I2A attack than adversarially trained models. For example, the undefended ConvNeXt-L model achieves 9.32% accuracy under I2A attack while the adversarially trained model from [45] only achieves 4.95% accuracy. However, this phenomenon is not observed for the baseline attacks. We believe this is because the adversarial examples generated by I2A lie on the natural image manifold, while adversarial training hurts the model performance on natural images [64] as indicated by the degraded performance on clean images.

I2A also remains much more effective under the strong preprocessing defense DiffPure [57] compared to the baseline attacks since I2A generates natural semantic perturbations that are less likely to be removed in the denoising diffusion process. For example, for the Swin-L model, I2A achieves 55.18% classification accuracy under the DiffPure defense, while the second best method Fog [33] achieves 73.56% accuracy, which is 18.38% higher than I2A. Note that the results of DiffPure in Table 1 are under non-adaptive attacks where the attacker does not attempt to attack the defense mechanism. We further investigate the adaptive attack scenario, where the attacker uses the BPDA+EOT techniques [5, 77] to attack the DiffPure defense. Due to the high computational cost, we experiment with 200 images, and for I2A attack we use the prompt "make it in snow". The results are summarized in Table 2. I2A can successfully break the DiffPure defense under the adaptive attack setting, bringing down the accuracy to as low as 7.0%. However, DiffPure demonstrates strong robustness the noise-based PGD [54] even under strong adaptive attacks, *e.g.*, achieving 68.5% accuracy for the Swin-B model. StAdv [81] is a semantic attack based on local geometric transformations, which is more effective than PGD in attacking DiffPure, but still performs worse than I2A.

Black-box attack. We also consider the black-box attack scenarios where we craft the attacks on a source model and

Model	Method	Clean	FGSM	PGD	MIM	Auto	Fog	Gabor	Snow	StAdv	PerC-AL	I2A (Ours)
ResNet-18	Undefended	69.68	0.90	0.00	0.00	0.00	5.24	0.20	0.26	0.00	56.16	1.20
	Salman2020 [68]	52.92	32.54	29.77	29.84	25.32	27.14	33.44	30.46	29.40	<u>9.92</u>	0.54
	DiffPure [57]	64.70	58.98	62.16	61.36	63.22	51.20	59.84	53.34	<u>49.58</u>	64.74	42.47
ResNet-50	Undefended	76.52	5.96	0.00	0.00	0.00	6.76	0.04	1.12	0.00	72.34	2.11
	Salman2020 [68]	64.02	43.44	38.98	39.06	34.96	36.22	41.44	40.36	36.56	<u>18.68</u>	1.42
	Engstrom2019 [18]	62.56	39.92	32.92	33.18	29.22	37.30	37.24	37.94	36.46	<u>20.96</u>	2.52
	FastAT [80]	55.62	32.84	27.94	26.26	26.24	19.54	30.76	27.28	31.90	<u>13.74</u>	1.29
	DiffPure [57]	70.54	66.94	69.16	68.06	69.68	58.90	66.42	61.62	<u>56.20</u>	70.48	46.87
ConvNeXt-B	Undefended	83.36	41.44	0.00	0.00	0.00	11.16	0.14	6.86	0.70	19.94	8.93
	ARES [45]	76.02	59.60	56.28	56.60	55.82	59.41	58.06	59.36	<u>47.56</u>	74.66	4.12
	ConvStem [71]	75.90	59.92	56.74	56.88	56.14	60.12	58.64	59.32	<u>49.56</u>	75.22	3.62
	DiffPure [57]	78.10	74.90	77.32	76.58	77.54	69.28	75.04	<u>54.82</u>	<u>70.92</u>	75.74	53.34
ConvNeXt-L	Undefended	83.62	44.44	0.00	0.00	0.00	9.38	0.18	6.72	1.60	16.08	9.32
	ARES [45]	78.02	62.00	58.60	58.76	58.48	60.52	60.78	61.74	<u>51.22</u>	77.02	4.95
	ConvStem [71]	77.00	60.58	57.70	58.00	57.70	60.28	59.96	60.54	<u>49.22</u>	76.62	4.91
	DiffPure [57]	78.68	75.12	77.84	77.02	78.12	<u>69.84</u>	75.32	73.66	<u>71.52</u>	78.12	52.71
Swin-B	Undefended	81.98	43.50	0.00	0.00	0.00	12.24	0.30	6.64	2.52	51.02	8.81
	ARES [45]	76.16	59.78	57.12	57.32	56.16	59.18	58.76	58.90	47.76	<u>41.06</u>	3.47
	DiffPure [57]	76.60	74.02	75.88	75.28	75.92	<u>68.64</u>	73.50	70.90	70.12	76.54	50.65
Swin-L	Undefended	85.06	45.72	0.00	0.00	0.00	6.92	0.78	8.72	2.96	57.62	8.40
	ARES [45]	78.92	62.84	59.44	59.72	59.56	60.82	61.60	62.34	<u>51.62</u>	62.56	4.98
	DiffPure [57]	81.40	79.56	80.66	80.26	81.02	<u>73.56</u>	78.72	75.9	<u>74.48</u>	80.92	55.18
Average Accuracy		73.97	51.13	41.75	41.55	41.14	41.98	42.33	41.76	<u>37.81</u>	54.00	16.90

Table 1. **White-box attacks.** We report top-1 (%) on ImageNet. The best for defended models are in **bold** and the 2nd best are underlined.

Model	Adaptive	Clean	PGD	StAdv	I2A (Ours)
ResNet-18	✗	70.0	68.5	<u>57.0</u>	43.5
	✓	70.0	44.0	<u>34.0</u>	7.0
ResNet-50	✗	75.0	75.0	<u>59.0</u>	52.5
	✓	75.0	56.0	<u>40.5</u>	9.0
Swin-B	✗	80.0	75.5	<u>69.0</u>	52.0
	✓	80.0	68.5	<u>52.5</u>	20.5

Table 2. **DiffPure defense under adaptive and non-adaptive attacks** [57]. We report top-1 (%) on ImageNet.

evaluate them on the target models. The results are presented in Fig. 4, where we show the transferability within undefended models as well as adversarially trained models. For adversarially trained models, we use models trained by [68] for ResNet-18 and ResNet-50, and models trained by [45] for the other network architectures. In general, attacks crafted on stronger models such as Swin-B and Swin-L tend to transfer better to weaker models such as ResNet-18 and ResNet-50, indicated by lower values in the lower triangles than the upper triangles of the figures. In addition, the attacks seem to transfer better within adversarially trained models than undefended models, resulting in lower classification accuracy. Overall, semantic attacks such as I2A and StAdv [81] achieve better transferability than noise-based attacks such as PGD [54] and AutoAttack [12]. For undefended models, I2A achieves slightly

higher average classification accuracy than StAdv (57.15% vs. 54.71%). However, I2A obtains much lower average classification accuracy than StAdv for adversarially trained models (39.90% vs. 60.75%), indicating better transferability of I2A. In particular, the I2A attack crafted on Swin-L achieves 17.42% accuracy when evaluated on ResNet-18, resulting in a black-box attack success rate of **82.58%**. The great transferability of I2A suggests that it captures the common vulnerabilities among different models.

Visualization. In Fig. 5, we present adversarial images produced by the various attack methods. PGD [54] generates adversarial images by adding subtle adversarial noise, which creates unnatural adversarial patterns on the image. Fog and Snow attacks [33] introduce adversarially chosen partial occlusion of the image to mimic the effect of mist and snowflakes, yet these perturbations appear artificial. Gabor attack [33] superimposes adversarial Gabor noise onto the image, which is conspicuous and compromises image quality. Perc-AL [90] minimizes perturbation sizes with respect to perceptual color distance, resulting in large yet imperceptible perturbations, but the attack strength is relatively weak as shown in Table 1. StAdv attack [81] introduces adversarial local geometric transformations which distort the input image. The proposed I2A attack generates natural and diverse perturbations based on the text instructions, resulting in visually appealing adversarial images. More visualizations can be found in the Supp.

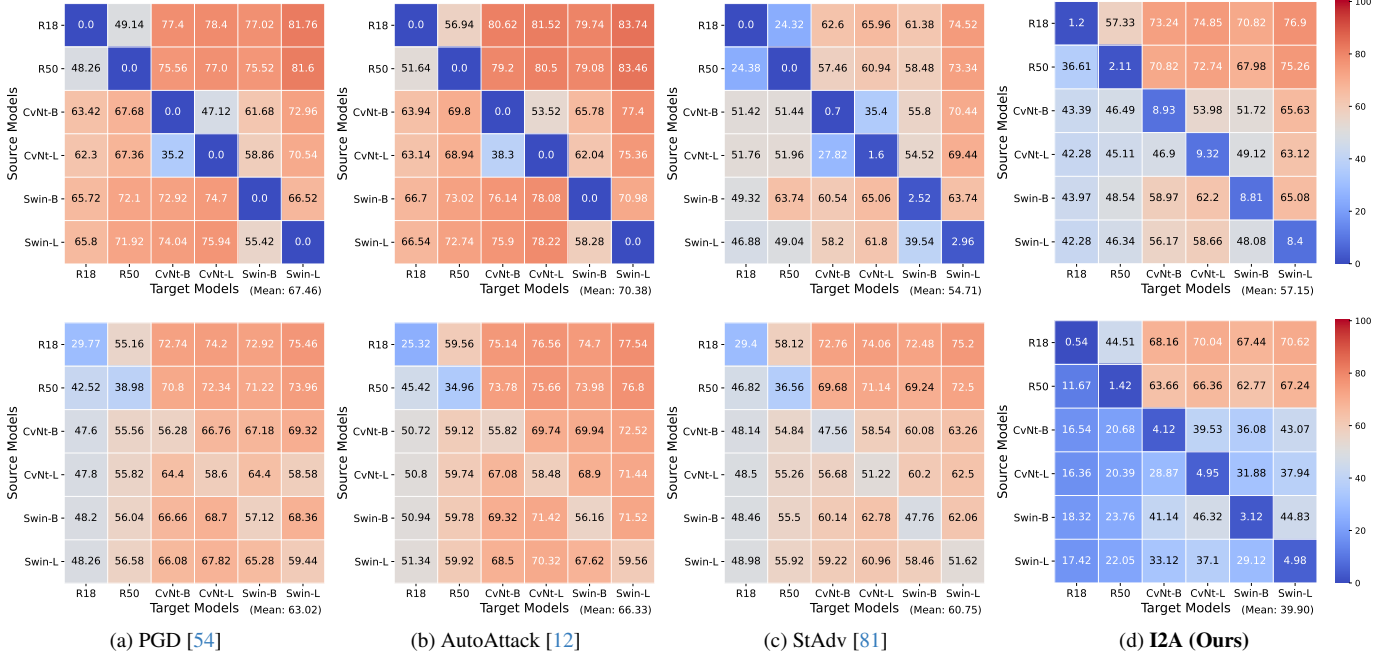


Figure 4. **Black-box attacks.** We report top-1 (%) on ImageNet. *Top*: transferability between undefended models. *Bottom*: transferability between adversarially trained models. Average accuracy of black-box attacks is marked on the bottom right of each figure.

Model	Method	Clean	PGD	StAdv	I2A
ResNet-18	Undefended	52.96	0.0	0.17	0.41
	DiffPure [57]	50.88	44.63	<u>36.26</u>	26.68
ResNet-50	Undefended	53.70	0.0	0.10	0.61
	DiffPure [57]	52.25	47.86	<u>39.51</u>	29.06
DenseNet-161	Undefended	54.50	0.0	0.27	0.73
	DiffPure [57]	51.69	48.75	<u>40.31</u>	30.71
Average Accuracy		52.66	23.54	<u>19.44</u>	14.70

Table 3. **White-box attacks on Places365.** We report top-1 (%). The best for DiffPure are in **bold** and the 2nd best are underlined.

4.3. Results on Places365

To demonstrate the generalizability of our method to different data domains, we also evaluate I2A on Places365 [91]. The results are shown in Table 3. We compare I2A to PGD [54] and StAdv [61] attacks. All three methods can break the undefended models, bringing down the classification accuracy to almost zero. However, I2A achieves much lower classification accuracy when the DiffPure defense is used. Visualizations of Places365 can be found in the Supp.

4.4. Ablation Studies

We conduct ablations on a subset of 500 images on the undefended models. We use the prompt "make it in snow". The other settings are the same as those in Sec. 4.1.

Effect of adversarial diffusion guidance. We demonstrate the effect of the adversarial guidance factors α and

α	β	R-18	R-50	CvNt-B	CvNt-L	Swin-B	Swin-L
\times	\times	64.0	71.6	81.0	81.4	79.8	82.4
\times	\checkmark	24.8	30.4	50.0	51.6	48.0	54.2
\checkmark	\times	<u>19.0</u>	<u>25.4</u>	<u>33.4</u>	<u>35.4</u>	<u>32.6</u>	<u>36.0</u>
\checkmark	\checkmark	2.0	2.0	11.2	13.4	10.0	8.8
Clean		69.6	77.4	84.2	84.0	81.6	82.4

Table 4. **Classification accuracy (%) under different adversarial diffusion guidance.** R-18/50 denotes the ResNet-18/50 networks and CvNt-B/L denotes the ConvNext-B/L networks.

β of Eq. (3) in Table 4. When we do not apply α and β (row 1), which is the benign editing setting, the classification accuracies are similar to these on clean images. When we introduce β to the text guidance term (row 2) or α to the image guidance term (row 3), the classification accuracies drop significantly. In addition, it can be observed that modulating the image guidance term is more effective than the text guidance term by comparing row 2 with row 3. The attacks are most effective when we apply both α and β . These results demonstrate the effectiveness of the proposed adversarial diffusion guidance method.

Effect of perceptual constraint. We use the LPIPS distance to bound the adversarial perturbations with a budget of γ . We show the effect of different γ in Table 5 with ResNet-18 as the victim model. $\gamma = 1$ corresponds to the unbounded case. As γ increases, we have stronger attacks but lower FID [26], which indicates lower image quality. Furthermore, a high γ could lead to failures of semantic editing as shown in Fig. 6. We set $\gamma = 0.3$ since it achieves

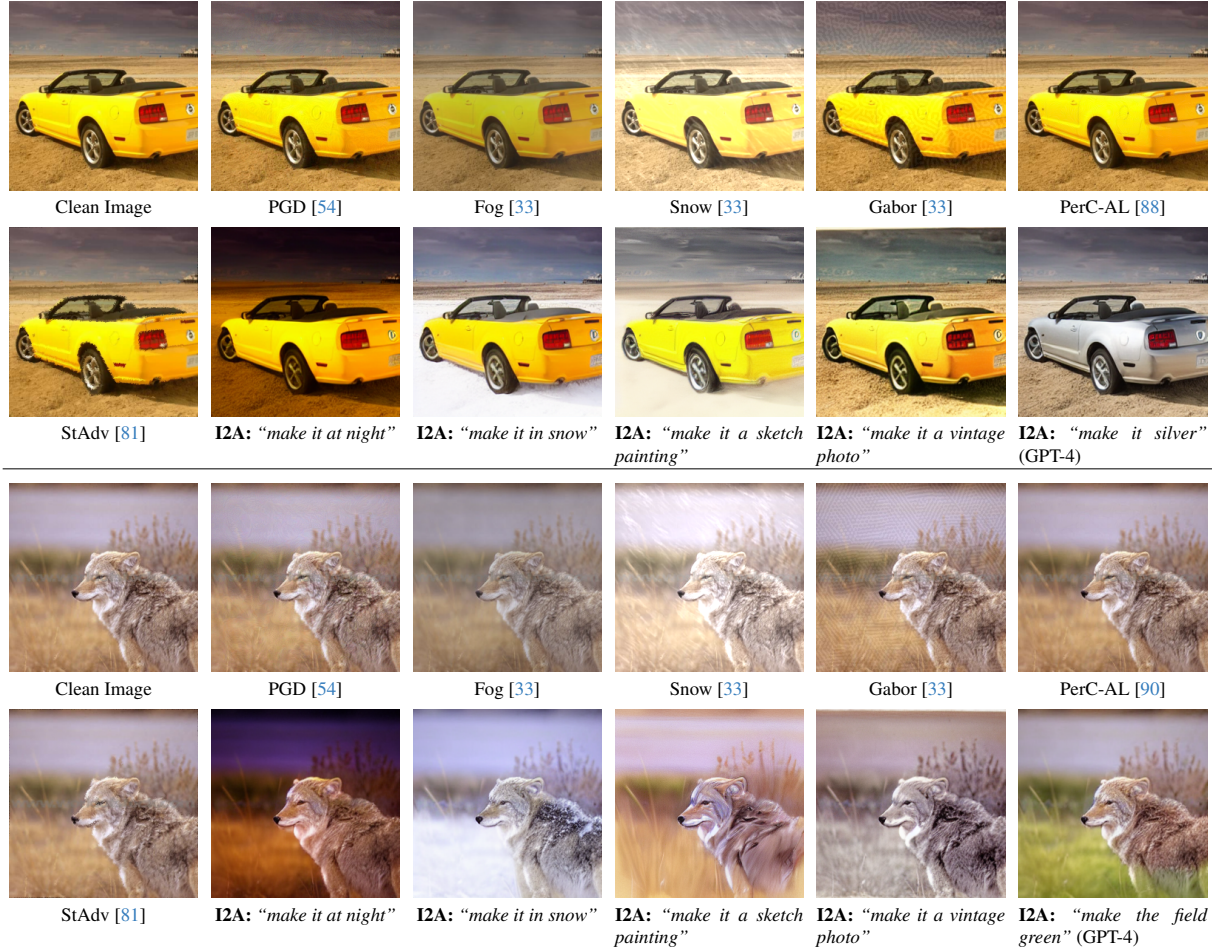


Figure 5. **Visualization of adversarial images.** I2A generates natural and diverse perturbations based on the text instructions.

γ	0.1	0.2	0.3	0.5	0.7	1.0
Accuracy (%)	15.6	3.6	2.0	0.2	0.2	0.2
FID	34.71	44.03	56.72	73.35	80.83	82.28

Table 5. **Effect of γ .**

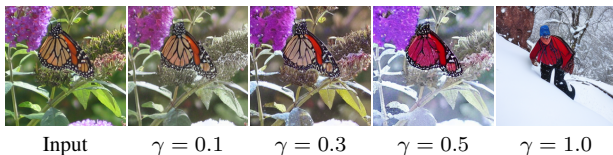


Figure 6. **Visualization** of adversarial samples with different γ .

a nice tradeoff between image quality and attack performance. In addition, the average LPIPS distance between benign edited images and the original images is 0.29, which suggests that $\gamma = 0.3$ is a reasonable LPIPS bound.

5. Discussion and Conclusion

In this work, we propose Instruct2Attack (I2A), a language-guided semantic attack that performs adversarial semantic editing on the input image based on the language instruction. I2A leverages a pretrained conditional latent diffusion

model and adversarially guides the reverse diffusion process to search for an adversarial code in the latent space. The adversarial perturbation is bounded by the LPIPS distance to ensure the similarity between the input image and the adversarial image. We further explore to use GPT-4 to automatically generate diverse and image-specific instructions. Extensive experiments demonstrate the superiority of I2A under both white-box and black-box settings.

The perturbations generated by I2A are natural, semantically meaningful, and interpretable. I2A reveals the vulnerabilities of DNNs under common natural semantic modifications. The success of I2A suggests the ubiquity of adversarial examples on the image manifold. Since on-manifold adversarial examples are generalization errors [74], we believe the failures caused by I2A reflect the biases in datasets where certain semantic combinations are less common, such as nighttime and snowy scenes. I2A can serve as a flexible tool for evaluating model robustness under various semantic changes and diagnosing model failure modes. It can also be used as a data augmentation technique to generate synthetic training samples to enhance model robustness.

Acknowledgment This work was partially supported by the DARPA GARD Program HR001119S0026-GARD-FP-052. Jiang Liu acknowledges support through a fellowship from JHU + Amazon Initiative for Interactive AI (AI2AI).

References

- [1] Rameen Abdal, Yipeng Qin, and Peter Wonka. Image2StyleGAN: How to embed images into the StyleGAN latent space? In *ICCV*, 2019. 2
- [2] Rameen Abdal, Yipeng Qin, and Peter Wonka. Image2StyleGAN++: How to edit the embedded images? In *CVPR*, 2020. 2
- [3] Naveed Akhtar and Ajmal Mian. Threat of adversarial attacks on deep learning in computer vision: A survey. *IEEE Access*, 2018. 1
- [4] Yuval Alaluf, Omer Tov, Ron Mokady, Rinon Gal, and Amit Bermano. HyperStyle: StyleGAN Inversion with HyperNetworks for Real Image Editing. In *CVPR*, 2022. 2
- [5] Anish Athalye, Nicholas Carlini, and David Wagner. Obfuscated gradients give a false sense of security: Circumventing defenses to adversarial examples. In *ICLR*, 2018. 5
- [6] Omri Avrahami, Dani Lischinski, and Ohad Fried. Blended diffusion for text-driven editing of natural images. In *CVPR*, 2022. 2
- [7] Anand Bhattad, Min Jin Chong, Kaizhao Liang, Bo Li, and D. A. Forsyth. Unrestricted adversarial examples via semantic manipulation. In *ICLR*, 2020. 2
- [8] Tim Brooks, Aleksander Holynski, and Alexei A Efros. InstructPix2Pix: Learning to Follow Image Editing Instructions. *CVPR*, 2023. 2, 3, 5, 1
- [9] Nicholas Carlini and David Wagner. Towards evaluating the robustness of neural networks. In *IEEE Symposium on Security and Privacy*, 2017. 1, 2, 3
- [10] Lucy Chai, Jonas Wulff, and Phillip Isola. Using latent space regression to analyze and leverage compositionality in gans. In *ICLR*, 2021. 2
- [11] Jianqi Chen, Hao Chen, Keyan Chen, Yilan Zhang, Zhengxia Zou, and Zhenwei Shi. Diffusion models for imperceptible and transferable adversarial attack. *arXiv preprint arXiv:2305.08192*, 2023. 2
- [12] Francesco Croce and Matthias Hein. Reliable evaluation of adversarial robustness with an ensemble of diverse parameter-free attacks. In *ICML*, 2020. 5, 6, 7, 1
- [13] Francesco Croce, Maksym Andriushchenko, Vikash Sehwag, Edoardo Debenedetti, Nicolas Flammarion, Mung Chiang, Prateek Mittal, and Matthias Hein. Robustbench: a standardized adversarial robustness benchmark. In *NeurIPS*, 2021. 2, 5
- [14] Katherine Crowson, Stella Biderman, Daniel Kornis, Dashiell Stander, Eric Hallahan, Louis Castricato, and Edward Raff. VQGAN-CLIP: Open domain image generation and editing with natural language guidance. In *ECCV*, 2022. 2
- [15] Jia Deng, Wei Dong, Richard Socher, Li-Jia Li, Kai Li, and Li Fei-Fei. Imagenet: A large-scale hierarchical image database. In *CVPR*, 2009. 5, 3
- [16] Yinpeng Dong, Fangzhou Liao, Tianyu Pang, Hang Su, Jun Zhu, Xiaolin Hu, and Jianguo Li. Boosting adversarial attacks with momentum. In *CVPR*, 2018. 5, 1
- [17] Yinpeng Dong, Shouwei Ruan, Hang Su, Caixin Kang, Xingxing Wei, and Jun Zhu. Viewfool: Evaluating the robustness of visual recognition to adversarial viewpoints. In *NeurIPS*, 2022. 2
- [18] Logan Engstrom, Andrew Ilyas, Shibani Santurkar, Dimitris Tsipras, Brandon Tran, and Aleksander Madry. Learning perceptually-aligned representations via adversarial robustness. In *ArXiv preprint arXiv:1906.00945*, 2019. 2, 5, 6, 4
- [19] Logan Engstrom, Brandon Tran, Dimitris Tsipras, Ludwig Schmidt, and Aleksander Madry. A rotation and a translation suffice: Fooling CNNs with simple transformations. 2019. 2
- [20] Rinon Gal, Or Patashnik, Haggai Maron, Amit H Bermano, Gal Chechik, and Daniel Cohen-Or. StyleGAN-NADA: Clip-guided domain adaptation of image generators. *ACM Transactions on Graphics (TOG)*, 41(4):1–13, 2022. 2
- [21] Ross B. Girshick, Jeff Donahue, Trevor Darrell, and Jitendra Malik. Rich feature hierarchies for accurate object detection and semantic segmentation. *CVPR*, 2013. 1
- [22] Ian Goodfellow, Jean Pouget-Abadie, Mehdi Mirza, Bing Xu, David Warde-Farley, Sherjil Ozair, Aaron Courville, and Yoshua Bengio. Generative adversarial nets. *NeurIPS*, 2014. 2
- [23] Ian J Goodfellow, Jonathon Shlens, and Christian Szegedy. Explaining and harnessing adversarial examples. In *ICLR*, 2015. 1, 2, 3, 5
- [24] Kaiming He, Xiangyu Zhang, Shaoqing Ren, and Jian Sun. Deep residual learning for image recognition. In *CVPR*, 2016. 5
- [25] Amir Hertz, Ron Mokady, Jay Tenenbaum, Kfir Aberman, Yael Pritch, and Daniel Cohen-or. Prompt-to-Prompt Image Editing with Cross-Attention Control. In *ICLR*, 2023. 2
- [26] Martin Heusel, Hubert Ramsauer, Thomas Unterthiner, Bernhard Nessler, and Sepp Hochreiter. GANs trained by a two time-scale update rule converge to a local nash equilibrium. In *NeurIPS*, 2017. 7
- [27] Jonathan Ho and Tim Salimans. Classifier-free diffusion guidance. In *NeurIPS 2021 Workshop on Deep Generative Models and Downstream Applications*, 2021. 3
- [28] Jonathan Ho, Ajay Jain, and Pieter Abbeel. Denoising diffusion probabilistic models. *NeurIPS*, 2020. 2
- [29] Hossein Hosseini and Radha Poovendran. Semantic adversarial examples. In *CVPRW*, 2018. 2
- [30] Phillip Isola, Jun-Yan Zhu, Tinghui Zhou, and Alexei A Efros. Image-to-image translation with conditional adversarial networks. In *CVPR*, 2017. 2
- [31] Ajil Jalal, Andrew Ilyas, Constantinos Daskalakis, and Alexandros G Dimakis. The robust manifold defense: Adversarial training using generative models. *arXiv preprint arXiv:1712.09196*, 2017. 2
- [32] Ameya Joshi, Amitangshu Mukherjee, Soumik Sarkar, and Chinmay Hegde. Semantic adversarial attacks: Parametric transformations that fool deep classifiers. In *ICCV*, 2019. 1, 2

- [33] Daniel Kang, Yi Sun, Dan Hendrycks, Tom Brown, and Jacob Steinhardt. Testing robustness against unforeseen adversaries. *arXiv preprint arXiv:1908.08016*, 2019. 2, 5, 6, 8, 1, 7
- [34] Jacob Devlin Ming-Wei Chang Kenton and Lee Kristina Toutanova. Bert: Pre-training of deep bidirectional transformers for language understanding. In *Proceedings of NAACL-HLT*, pages 4171–4186, 2019. 2
- [35] Gwanghyun Kim, Taesung Kwon, and Jong Chul Ye. DiffusionCLIP: Text-guided diffusion models for robust image manipulation. In *CVPR*, 2022. 2
- [36] Alex Krizhevsky, Ilya Sutskever, and Geoffrey E Hinton. Imagenet classification with deep convolutional neural networks. In *NeurIPS*, 2012. 1, 5
- [37] Cassidy Laidlaw and Soheil Feizi. Functional adversarial attacks. *NeurIPS*, 2019. 2
- [38] Cassidy Laidlaw, Sahil Singla, and Soheil Feizi. Perceptual adversarial robustness: Defense against unseen threat models. In *ICLR*, 2021. 2, 4, 3
- [39] Chun Pong Lau, Jiang Liu, and Rama Chellappa. Attribute-guided encryption with facial texture masking. *arXiv preprint arXiv:2305.13548*, 2023. 2
- [40] Chun Pong Lau, Jiang Liu, Wei An Lin, Hossein Souri, Pirazh Khorramshahi, and Rama Chellappa. Adversarial attacks and robust defenses in deep learning. In *Deep Learning*, pages 29–58. Elsevier BV, 2023. 2
- [41] Chun Pong Lau, Jiang Liu, Hossein Souri, Wei-An Lin, Soheil Feizi, and Rama Chellappa. Interpolated joint space adversarial training for robust and generalizable defenses. *PAMI*, 2023. 2
- [42] Junnan Li, Dongxu Li, Silvio Savarese, and Steven Hoi. BLIP-2: Bootstrapping language-image pre-training with frozen image encoders and large language models. In *ICML*, 2023. 4, 3
- [43] Wei-An Lin, Chun Pong Lau, Alexander Levine, Rama Chellappa, and Soheil Feizi. Dual Manifold Adversarial Robustness: Defense against Lp and non-Lp Adversarial Attacks. In *NeurIPS*, 2020. 2
- [44] Huan Ling, Karsten Kreis, Daiqing Li, Seung Wook Kim, Antonio Torralba, and Sanja Fidler. EditGAN: High-precision semantic image editing. In *NeurIPS*, 2021. 2
- [45] Chang Liu, Yinpeng Dong, Wenzhao Xiang, Xiao Yang, Hang Su, Jun Zhu, Yuefeng Chen, Yuan He, Hui Xue, and Shibao Zheng. A comprehensive study on robustness of image classification models: Benchmarking and rethinking. *arXiv preprint arXiv:2302.14301*, 2023. 2, 5, 6, 4
- [46] Hsueh-Ti Derek Liu, Michael Tao, Chun-Liang Li, Derek Nowrouzezahrai, and Alec Jacobson. Beyond pixel norm-balls: Parametric adversaries using an analytically differentiable renderer. In *ICLR*, 2018. 2
- [47] Jiang Liu, Chun Pong Lau, Hossein Souri, Soheil Feizi, and Rama Chellappa. Mutual adversarial training: Learning together is better than going alone. *IEEE Transactions on Information Forensics and Security*, 2022. 2
- [48] Jiang Liu, Alexander Levine, Chun Pong Lau, Rama Chellappa, and Soheil Feizi. Segment and complete: Defending object detectors against adversarial patch attacks with robust patch detection. In *CVPR*, 2022. 2
- [49] Jiang Liu, Chun Pong Lau, and Rama Chellappa. Diff-protect: Generate adversarial examples with diffusion models for facial privacy protection. *arXiv preprint arXiv:2305.13625*, 2023. 2
- [50] Ze Liu, Yutong Lin, Yue Cao, Han Hu, Yixuan Wei, Zheng Zhang, Stephen Lin, and Baining Guo. Swin transformer: Hierarchical vision transformer using shifted windows. In *CVPR*, 2021. 2, 5
- [51] Zhuang Liu, Hanzi Mao, Chao-Yuan Wu, Christoph Feichtenhofer, Trevor Darrell, and Saining Xie. A ConvNet for the 2020s. In *CVPR*, 2022. 5
- [52] Wuyang Luo, Su Yang, Hong Wang, Bo Long, and Weishan Zhang. Context-consistent semantic image editing with style-preserved modulation. In *ECCV*, 2022. 2
- [53] Wuyang Luo, Su Yang, Xinjian Zhang, and Weishan Zhang. SIEDOB: Semantic Image Editing by Disentangling Object and Background. In *CVPR*, 2023. 2
- [54] Aleksander Madry, Aleksandar Makelov, Ludwig Schmidt, Dimitris Tsipras, and Adrian Vladu. Towards deep learning models resistant to adversarial attacks. In *ICLR*, 2018. 1, 2, 3, 5, 6, 7, 8
- [55] Alexander Quinn Nichol and Prafulla Dhariwal. Improved denoising diffusion probabilistic models. In *ICML*, 2021. 2
- [56] Alexander Quinn Nichol, Prafulla Dhariwal, Aditya Ramesh, Pranav Shyam, Pamela Mishkin, Bob McGrew, Ilya Sutskever, and Mark Chen. GLIDE: Towards Photorealistic Image Generation and Editing with Text-Guided Diffusion Models. In *ICML*, 2022. 2
- [57] Weili Nie, Brandon Guo, Yujia Huang, Chaowei Xiao, Arash Vahdat, and Anima Anandkumar. Diffusion models for adversarial purification. In *ICML*, 2022. 2, 5, 6, 7, 3, 4
- [58] Evangelos Ntavelis, Andrés Romero, Iason Kastanis, Luc Van Gool, and Radu Timofte. Sesame: Semantic editing of scenes by adding, manipulating or erasing objects. In *ECCV*, 2020. 2
- [59] OpenAI. GPT-4 technical report. *arXiv*, pages 2303–08774, 2023. 2, 4, 3
- [60] Taesung Park, Ming-Yu Liu, Ting-Chun Wang, and Jun-Yan Zhu. Semantic image synthesis with spatially-adaptive normalization. In *CVPR*, 2019. 2
- [61] Haonan Qiu, Chaowei Xiao, Lei Yang, Xinchun Yan, Honglak Lee, and Bo Li. Semanticadv: Generating adversarial examples via attribute-conditioned image editing. In *ECCV*, 2020. 1, 2, 7
- [62] Alec Radford, Luke Metz, and Soumith Chintala. Unsupervised representation learning with deep convolutional generative adversarial networks. *arXiv preprint arXiv:1511.06434*, 2015. 2
- [63] Alec Radford, Jong Wook Kim, Chris Hallacy, Aditya Ramesh, Gabriel Goh, Sandhini Agarwal, Girish Sastry, Amanda Askell, Pamela Mishkin, Jack Clark, et al. Learning transferable visual models from natural language supervision. In *ICML*, 2021. 2
- [64] Aditi Raghunathan, Sang Michael Xie, Fanny Yang, John C. Duchi, and Percy Liang. Understanding and mitigating the tradeoff between robustness and accuracy. In *ICML*, 2020. 5

- [65] Elad Richardson, Yuval Alaluf, Or Patashnik, Yotam Nitzan, Yaniv Azar, Stav Shapiro, and Daniel Cohen-Or. Encoding in style: a stylegan encoder for image-to-image translation. In *CVPR*, 2021. 2
- [66] Robin Rombach, Andreas Blattmann, Dominik Lorenz, Patrick Esser, and Björn Ommer. High-resolution image synthesis with latent diffusion models. In *CVPR*, 2022. 2, 3
- [67] Olaf Ronneberger, Philipp Fischer, and Thomas Brox. U-Net: Convolutional networks for biomedical image segmentation. In *MICCAI*, 2015. 3
- [68] Hadi Salman, Andrew Ilyas, Logan Engstrom, Ashish Kapoor, and Aleksander Madry. Do adversarially robust ImageNet models transfer better? In *NeurIPS*, 2020. 2, 5, 6, 4
- [69] Fahad Shamshad, Muzammal Naseer, and Karthik Nandakumar. CLIP2Protect: Protecting Facial Privacy using Text-Guided Makeup via Adversarial Latent Search. In *CVPR*, 2023. 2
- [70] Karen Simonyan and Andrew Zisserman. Very deep convolutional networks for large-scale image recognition. In *ICLR*, 2015. 1
- [71] Naman D Singh, Francesco Croce, and Matthias Hein. Revisiting Adversarial Training for ImageNet: Architectures, Training and Generalization across Threat Models. In *NeurIPS*, 2023. 2, 5, 6, 4
- [72] Jascha Sohl-Dickstein, Eric Weiss, Niru Maheswaranathan, and Surya Ganguli. Deep unsupervised learning using nonequilibrium thermodynamics. In *ICML*, 2015. 2
- [73] Yang Song, Jascha Sohl-Dickstein, Diederik P Kingma, Abhishek Kumar, Stefano Ermon, and Ben Poole. Score-based generative modeling through stochastic differential equations. In *ICLR*, 2021. 3
- [74] David Stutz, Matthias Hein, and Bernt Schiele. Disentangling adversarial robustness and generalization. In *CVPR*, 2019. 8
- [75] Christian Szegedy, Wojciech Zaremba, Ilya Sutskever, Joan Bruna, Dumitru Erhan, Ian Goodfellow, and Rob Fergus. Intriguing properties of neural networks. *ICLR*, 2014. 1
- [76] Hao Tang, Dan Xu, Yan Yan, Philip HS Torr, and Nicu Sebe. Local class-specific and global image-level generative adversarial networks for semantic-guided scene generation. In *CVPR*, 2020. 2
- [77] Florian Tramer, Nicholas Carlini, Wieland Brendel, and Aleksander Madry. On adaptive attacks to adversarial example defenses. In *NeurIPS*, 2020. 5
- [78] Ashish Vaswani, Noam Shazeer, Niki Parmar, Jakob Uszkoreit, Llion Jones, Aidan N Gomez, Łukasz Kaiser, and Illia Polosukhin. Attention is all you need. *NeurIPS*, 2017. 3
- [79] Chenan Wang, Jinhao Duan, Chaowei Xiao, Edward Kim, Matthew Stamm, and Kaidi Xu. Semantic adversarial attacks via diffusion models. *arXiv preprint arXiv:2309.07398*, 2023. 2
- [80] Eric Wong, Leslie Rice, and J. Zico Kolter. Fast is better than free: Revisiting adversarial training. In *ICLR*, 2020. 2, 5, 6, 4
- [81] Chaowei Xiao, Jun-Yan Zhu, Bo Li, Warren He, Mingyan Liu, and Dawn Song. Spatially transformed adversarial examples. In *ICLR*, 2018. 2, 5, 6, 7, 8, 1
- [82] Xiaojun Xu, Xinyun Chen, Chang Liu, Anna Rohrbach, Trevor Darell, and Dawn Song. Can you fool AT with adversarial examples on a visual Turing test. *arXiv preprint arXiv:1709.08693*, 3, 2017. 2
- [83] Haotian Xue, Alexandre Araujo, Bin Hu, and Yongxin Chen. Diffusion-based adversarial sample generation for improved stealthiness and controllability. *arXiv preprint arXiv:2305.16494*, 2023. 2
- [84] Jongmin Yoon, Sung Ju Hwang, and Juho Lee. Adversarial purification with score-based generative models. In *ICML*, 2021. 2
- [85] Jiahui Yu, Zhe Lin, Jimei Yang, Xiaohui Shen, Xin Lu, and Thomas S Huang. Generative image inpainting with contextual attention. In *CVPR*, 2018. 2
- [86] Jiahui Yu, Zhe Lin, Jimei Yang, Xiaohui Shen, Xin Lu, and Thomas S Huang. Free-form image inpainting with gated convolution. In *ICCV*, 2019. 2
- [87] Oguz Kaan Yüksel, Sebastian U Stich, Martin Jaggi, and Tatjana Chavdarova. Semantic perturbations with normalizing flows for improved generalization. In *ICCV*, 2021. 2
- [88] Richard Zhang, Phillip Isola, Alexei A Efros, Eli Shechtman, and Oliver Wang. The unreasonable effectiveness of deep features as a perceptual metric. In *CVPR*, 2018. 4, 8, 5, 6, 7
- [89] Shengyu Zhao, Jonathan Cui, Yilun Sheng, Yue Dong, Xiao Liang, Eric I Chang, and Yan Xu. Large scale image completion via co-modulated generative adversarial networks. *arXiv preprint arXiv:2103.10428*, 2021. 2
- [90] Zhengyu Zhao, Zhuoran Liu, and Martha Larson. Towards large yet imperceptible adversarial image perturbations with perceptual color distance. In *CVPR*, 2020. 5, 6, 8, 1, 7
- [91] Bolei Zhou, Agata Lapedriza, Aditya Khosla, Aude Oliva, and Antonio Torralba. Places: A 10 million image database for scene recognition. *PAMI*, 2017. 5, 7, 3
- [92] Jun-Yan Zhu, Taesung Park, Phillip Isola, and Alexei A Efros. Unpaired image-to-image translation using cycle-consistent adversarial networks. In *ICCV*, 2017. 2

Instruct2Attack: Language-Guided Semantic Adversarial Attacks

Supplementary Material

A. Additional Implementation Details

A.1. Experiment Settings

All experiments are conducted using the PyTorch framework. We fix the random seed of every experiment to avoid the randomness of diffusion sampling.

A.2. Projection Algorithm

At the end of the attack generation, we ensure the perceptual constraint is satisfied by projecting \mathbf{x}_{adv} back to the feasible set through dynamically adjusting s_I and s_T in Eq. (3) which control the trade-off between how strongly the edited image corresponds with the input image and the edit instruction. A higher s_I produces an image that is more faithful to the input image, while a higher s_T results in a stronger edit applied to the input. In this work, we use the default setting $s_I = 1.5$ and $s_T = 7.5$ suggested by [8]. To project the adversarial image \mathbf{x}_{adv} back to the LPIPS bound of γ , we first set $s_T = 0$ and gradually increase the value of s_I to find a value of s_I^* such that the resulting image satisfies the LPIPS bound. Then we aim to increase the value of s_T from 0 to find a s_T^* that is as large as possible using the bisection method such that the final projected image satisfies the perceptual constraint. To search for s_I^* , we set the maximum value $s_{I\text{max}}$ to 10, and the search step size η_{s_I} to 0.2. To calculate s_T^* , we use $n = 10$ iterations of the bisection method with the maximum value of s_T set to $s_{T\text{max}} = 20$. The projection algorithm is summarized in Algorithm 2.

A.3. Baseline Attacks

The implementation details for the baseline attacks are as follows:

- **FGSM** [75]: We use L_∞ norm with a bound of 4/255.
- **PGD** [54]: We use L_∞ norm with a bound of 4/255 with 100 iterations and step size 1/255.
- **MIM** [16]: We use L_∞ norm with a bound of 4/255 with 100 iterations, step size 1/255, and decay factor 1.0.
- **AutoAttack** [12]: We use L_∞ norm with a bound of 4/255 and use the standard version of AutoAttack¹.
- **Fog** [33]: We set the number of iterations to 200, ϵ to 128, and step size to 0.002236.
- **Snow** [33]: We set the number of iterations to 200, ϵ to 0.0625, and step size to 0.002236.
- **Gabor** [33]: We set the number of iterations to 200, ϵ to 12.5, and step size to 0.002236.
- **StAdv** [81]: We set the number of iterations to 200 with a bound of 0.005.

¹<https://github.com/fra31/auto-attack>

Algorithm 2 Perceptual Projection

```
1: Input:  $\mathbf{x}, \mathbf{T}, \mathbf{z}_T, \gamma, T, \epsilon_\theta, \mathcal{E}, \mathcal{D}, \mathcal{C}$ , optimized  $\alpha$  and  $\beta$ ,  
   initial  $s_I, s_{I\text{max}}, s_{T\text{max}}, \eta_{s_I}, n$ .  
2: Output: Projected adversarial image  $\tilde{\mathbf{x}}_{\text{adv}}$   
3:  $\triangleright$  Image and text encoding  
4:  $\mathbf{c}_I = \mathcal{E}(\mathbf{x}), \mathbf{c}_L = \mathcal{C}(\mathbf{L})$   
5:  $\triangleright$  Search for  $s_I^*$   
6:  $s_T \leftarrow 0$   
7: while  $s_I \leq s_{I\text{max}}$   
8:    $\tilde{\mathbf{z}} = \text{LDM}(\mathbf{z}_T; \mathbf{c}_I, \mathbf{c}_L, \alpha, \beta, s_I, s_T)$   $\triangleright$  Sample  $\tilde{\mathbf{z}}$   
9:    $\tilde{\mathbf{x}} = \mathcal{D}(\tilde{\mathbf{z}})$   $\triangleright$  Generate  $\tilde{\mathbf{x}}$   
10:  if  $d(\tilde{\mathbf{x}}, \mathbf{x}) \leq \gamma$   
11:     $s_I^* = s_I$   
12:    break  
13:  else  
14:     $s_I = s_I + \eta_{s_I}$   
15:  end if  
16: end while  
17:  $\triangleright$  Calculate  $s_T^*$   
18:  $s_{T\text{min}} \leftarrow 0$   
19: for  $i = 0$  to  $n$   
20:    $s_T = (s_{T\text{min}} + s_{T\text{max}})/2$   
21:    $\tilde{\mathbf{z}} = \text{LDM}(\mathbf{z}_T; \mathbf{c}_I, \mathbf{c}_L, \alpha, \beta, s_I^*, s_T)$   $\triangleright$  Sample  $\tilde{\mathbf{z}}$   
22:    $\tilde{\mathbf{x}} = \mathcal{D}(\tilde{\mathbf{z}})$   $\triangleright$  Generate  $\tilde{\mathbf{x}}$   
23:   if  $d(\tilde{\mathbf{x}}, \mathbf{x}) > \gamma$   
24:      $s_{T\text{max}} = s_T$   
25:   else  
26:      $s_{T\text{min}} = s_T, \tilde{\mathbf{x}}_{\text{adv}} = \tilde{\mathbf{x}}$   
27:   end if  
28: end for
```

- **PerC-AL** [90]: We follow the default settings in the official github repository², and set the maximum number of iterations to 1000, $\alpha_l = 1.0$, $\alpha_c = 0.5$, and $\kappa = 40$.

When applying EOT+BPDA attacks for adaptively attacking DiffPure in Sec. 4.2, we set the maximum number of iterations to 50 for all attacks including I2A due to the high computational cost.

A.4. Victim Models for ImageNet

The implementation details for the victim models of ImageNet are as follows:

- **Undefended Models:** For ResNet-18/50, we use the pre-trained models provided by torchvision. For Swin-B/L, we use the pretrained models provided in the official

²<https://github.com/ZhengyuZhao/PerC-Adversarial>

λ	10	50	100	150	200	500
Accuracy (%)	24.6	2.8	1.8	1.8	1.8	2.2
Failure (%)	28.8	1.4	0.0	0.2	0.4	0.2

Table A. **Effect of λ .** We report the top-1 accuracy and the failure rate where the LPIPS bound is not satisfied.

github repository³, with initial patch size of 4, window size of 7, and image size of 224. For ConvNext-B/L, we use the pretrained models provided in the official github repository⁴.

- **Adversarially Trained Models:** For adversarially trained models, we use the model weights provided by Robustbench [13].
- **DiffPure Defended Models:** We apply the DiffPure [57] defense to the undefended models. We follow the implementations of the official github repository⁵.

A.5. Victim Models for Places365

The implementation details for the victim models of Places365 are as follows:

- **Undefended Models:** We use the pretrained ResNet-18/50 and DenseNet-161 models provided by the official repository of Places365⁶.
- **DiffPure Defended Models:** We apply the DiffPure [57] defense to the undefended models.

B. More Quantitative Results

B.1. Effect of λ

We show the effect of the Lagrangian multiplier λ of Eq. (6) in Table A. A small λ fails to regularize the output to satisfy the perceptual constraint, resulting in a high failure rate. We chose $\lambda = 100$ since it achieves the lowest classification accuracy and failure rate.

B.2. Comparison with Neural Perceptual Attacks

By applying the perceptual constraint, I2A becomes a special case of the neural perceptual attacks (NPA) [38], which aims to find an adversarial example $\mathbf{x}_{\text{adv}} \in \mathcal{X}$ with a perceptual bound γ such that \mathbf{x}_{adv} is perceptually similar to \mathbf{x} but causes the classifier f to misclassify:

$$f(\mathbf{x}_{\text{adv}}) \neq y, \quad \text{and} \quad d(\mathbf{x}_{\text{adv}}, \mathbf{x}) \leq \gamma, \quad (8)$$

where d is the LPIPS distance, and y is the ground truth label. [38] proposed the Lagrangian Perceptual Attack (LPA) to solve for \mathbf{x}_{adv} by using a Lagrangian relaxation of the following constrained optimization problem:

³<https://github.com/microsoft/Swin-Transformer>

⁴<https://github.com/facebookresearch/ConvNeXt>

⁵<https://github.com/NVlabs/DiffPure>

⁶<https://github.com/CSAILVision/places365>

Model	Method	Clean	LPA	I2A
ResNet-18	Undefended	69.68	0.00	1.20
	Salman2020 [68]	52.92	0.00	0.54
	DiffPure [57]	64.70	61.98	42.47
ResNet-50	Undefended	76.52	0.00	2.11
	Salman2020 [68]	64.02	0.00	1.42
	Engstrom2019 [18]	62.56	0.02	2.52
	FastAT [80]	55.62	0.00	1.29
	DiffPure [57]	70.54	68.56	46.87
ConvNeXt-B	Undefended	83.36	0.00	8.93
	ARES [45]	76.02	0.18	4.12
	ConvStem [71]	75.90	0.78	3.62
	DiffPure [57]	78.10	75.94	53.34
ConvNeXt-L	Undefended	83.62	0.04	9.32
	ARES [45]	78.02	2.26	4.95
	ConvStem [71]	77.00	0.18	4.91
	DiffPure [57]	78.68	76.40	52.71
Swin-B	Undefended	81.98	0.00	8.81
	ARES [45]	76.16	0.82	3.47
	DiffPure [57]	76.60	75.00	50.65
Swin-L	Undefended	85.06	0.00	8.40
	ARES [45]	78.92	1.40	4.98
	DiffPure [57]	81.40	79.86	55.18
Average Accuracy		73.97	<u>20.16</u>	16.90

Table B. **Comparison with LPA under white-box attacks.** We report top-1 accuracy (%) on ImageNet under white-box attacks.

$$\max_{\mathbf{x}_{\text{adv}}} \mathcal{L}_m(\mathbf{x}_{\text{adv}}, y), \quad \text{s.t.}, \quad d(\mathbf{x}_{\text{adv}}, \mathbf{x}) \leq \gamma, \quad (9)$$

where \mathcal{L}_m is the margin loss from [9].

The main differences between LPA and I2A are as follows: 1) LPA is a *noise-based* attack that generates \mathbf{x}_{adv} by adding optimized adversarial noise to \mathbf{x} , while I2A is a *semantic* attack that generates semantically meaningful perturbation and constraints \mathbf{x}_{adv} to be *on-manifold*; 2) The adversarial noise generated by LPA lacks interpretability and naturalness, while I2A generates *interpretable* and *natural* adversarial images; 2) I2A is a *language-guided* attack that allows the user to control the adversarial perturbations through language instructions, while LPA does not provide such controllability and the resulting adversarial noise is purely driven by optimization.

We provide quantitative comparisons between I2A and LPA under white-box attacks in Table B. We set the perceptual bound to 0.3 for LPA and use the default settings of the official github repository⁷. LPA demonstrates strong attack ability on both undefended and adversarially trained models, resulting in nearly zero classification accuracy. However, since LPA is a noise-based attack, the adversarial noise

⁷<https://github.com/cassidyilaidlaw/perceptual-advex>

Model	Adaptive	Clean	LPA	I2A
ResNet-18	✗	70.0	67.5	43.5
	✓	70.0	34.0	7.0
ResNet-50	✗	75.0	74.5	52.5
	✓	75.0	46.0	9.0
Swin-B	✗	80.0	75.0	52.0
	✓	80.0	62.5	20.5

Table C. **DiffPure defense under adaptive and non-adaptive attacks [57].** We report top-1 (%) on ImageNet.

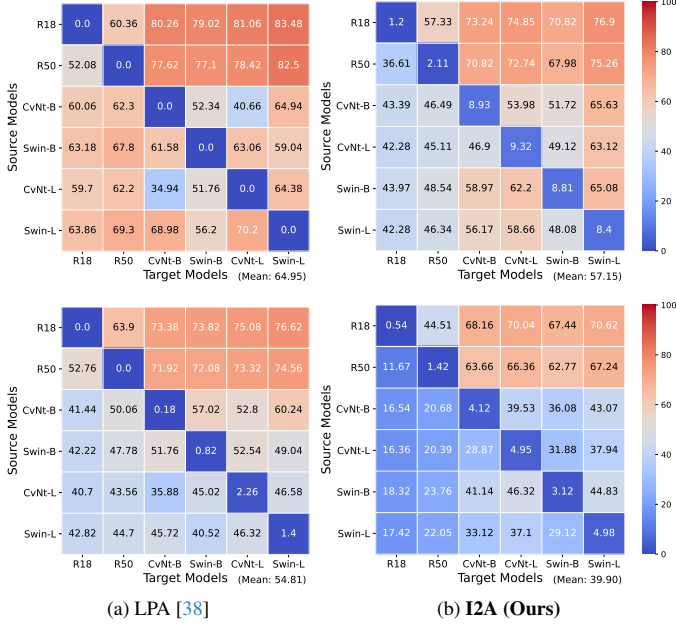


Figure A. **Black-box attacks.** We report top-1 (%) on ImageNet. *Top*: transferability between undefended models. *Bottom*: transferability between adversarially trained models. Average accuracy of black-box attacks is marked on the bottom right of each figure.

can be easily removed by DiffPure, resulting in much lower attack performance than I2A when the DiffPure defense is applied. We also apply the EOT+BPDA techniques for adaptively attacking DiffPure and the results are summarized in Table C. I2A achieves significantly better performance than LPA under the DiffPure defense, especially under the adaptive attack setting. In addition, I2A achieves much better transferability than LPA under black-box attacks, as shown in Fig. A. For example, I2A achieves an average of 39.90% classification accuracy for adversarially trained models, which is 14.91 points lower than LPA.

B.3. Performance of Each Prompt

We report the detailed performance of each prompt used by I2A in Table D. We use four manually written prompts and one GPT-4 generated prompt. The five prompts achieve

similar performance, which suggests the performance I2A is not sensitive to the input prompt. The prompt "make it a vintage photo" achieves slightly better performance compared to the others in terms of average accuracy.

C. More Visualization Results

We provide more visualization results on ImageNet [15] in Figs. B and C. We also provide visualization results on Places365 [91] in Figs. D and E. I2A generates diverse and natural adversarial images based on the language instructions, and generalizes well to different datasets.

D. Prompt for GPT-4

In this work, we propose to automatically generate image-specific editing instructions by first using BLIP-2 [42] to generate image captions and feed them into GPT-4 [59]. We utilize few-shot in-context learning by presenting 50 manually written examples in the prompt without fine-tuning the GPT-4 model. The prompt for GPT-4 to generate the edit instructions is presented in Table E.

Model	Method	Clean	snow	night	painting	vintage	GPT-4	Mean
ResNet-18	Undefended	69.68	0.82	0.94	0.38	<u>0.60</u>	3.26	1.20
	Salman2020 [68]	52.92	0.42	<u>0.28</u>	0.56	0.22	1.20	0.54
	DiffPure [57]	64.70	41.84	43.80	45.08	39.94	<u>41.70</u>	42.47
ResNet-50	Undefended	76.52	1.82	1.86	0.82	<u>0.96</u>	5.08	2.11
	Salman2020 [68]	64.02	1.46	0.90	1.24	<u>0.98</u>	2.52	1.42
	Engstrom2019 [18]	62.56	2.60	<u>2.20</u>	2.54	1.80	3.44	2.52
	FastAT [80]	55.62	1.24	<u>0.92</u>	1.44	0.90	1.94	1.29
	DiffPure [57]	70.54	47.68	47.48	49.42	44.00	<u>45.78</u>	46.87
ConvNeXt-B	Undefended	83.36	10.72	11.40	6.02	<u>6.42</u>	10.1	8.93
	ARES [45]	76.02	5.00	4.38	<u>3.00</u>	2.46	5.74	4.12
	ConvStem [71]	75.90	4.62	4.06	<u>2.20</u>	1.96	5.26	3.62
	DiffPure [57]	78.10	54.82	53.86	55.36	<u>51.58</u>	51.1	53.34
ConvNeXt-L	Undefended	83.62	11.50	11.60	<u>6.76</u>	6.14	10.62	9.32
	ARES [45]	78.02	6.24	5.00	<u>3.32</u>	3.30	6.88	4.95
	ConvStem [71]	77.00	6.16	5.38	<u>3.32</u>	3.04	6.66	4.91
	DiffPure [57]	78.68	53.86	53.92	53.56	<u>52.00</u>	50.22	52.71
Swin-B	Undefended	81.98	9.68	11.42	5.52	<u>6.12</u>	11.3	8.81
	ARES [45]	76.16	4.06	<u>3.18</u>	2.06	3.62	4.44	3.47
	DiffPure [57]	76.60	51.58	50.66	52.72	<u>49.26</u>	49.04	50.65
Swin-L	Undefended	85.06	8.94	9.84	<u>6.34</u>	6.04	10.84	8.40
	ARES [45]	78.92	5.90	4.98	3.56	<u>3.62</u>	6.84	4.98
	DiffPure [57]	81.40	57.18	55.88	55.68	<u>54.12</u>	53.02	55.18
Average Accuracy		73.97	17.64	17.45	<u>16.40</u>	15.41	17.59	16.90

Table D. **Effect of Prompts.** We report top-1 accuracy (%) on ImageNet under white-box attacks. We use four manually written prompts: "make it in snow" (snow), "make it at night" (night), "make it a sketch painting" (painting), and "make it a vintage photo" (vintage), as well as one prompt generated automatically by GPT-4. The best prompt of each row is in **bold** and the second best is underlined.

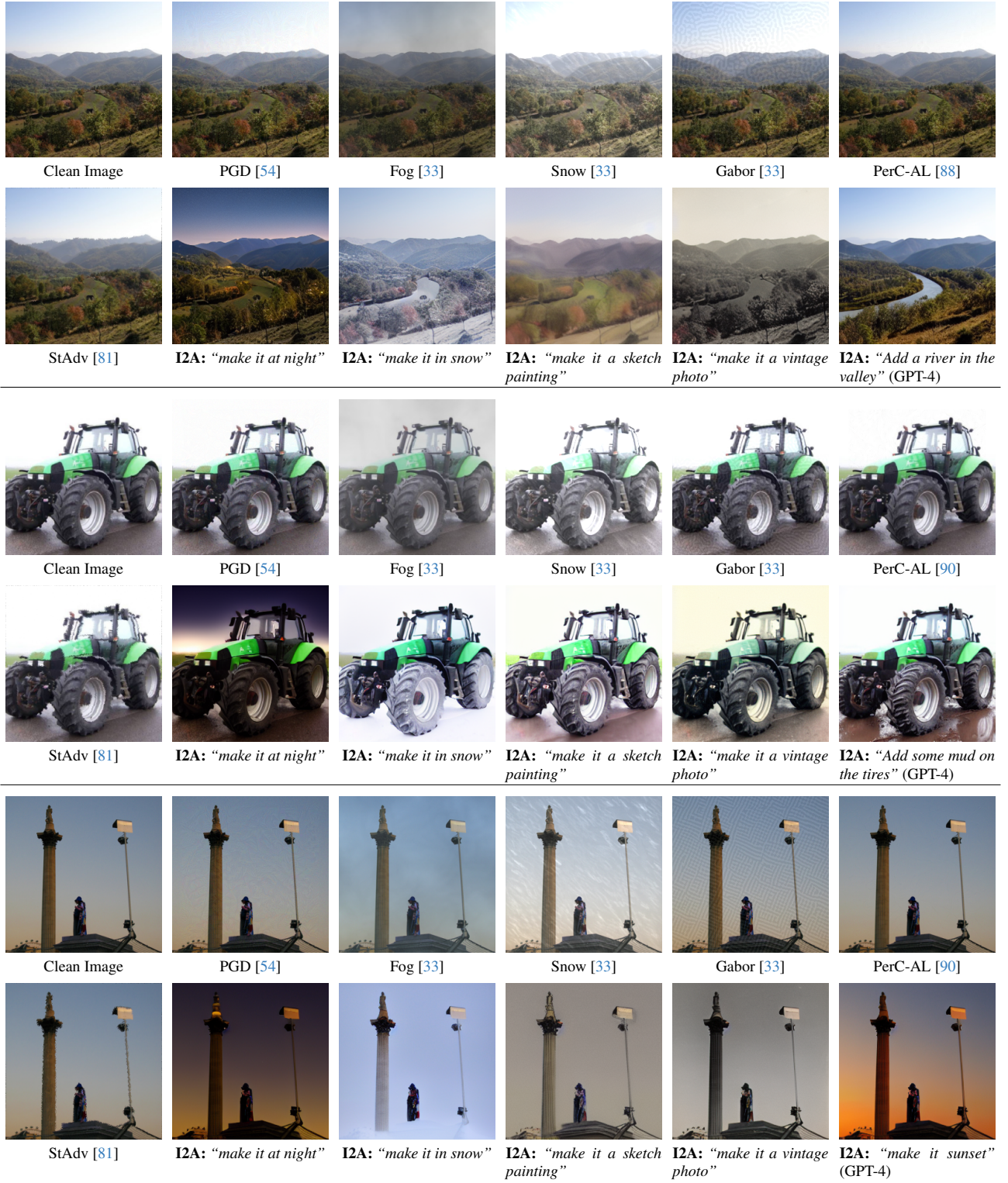


Figure B. **Visualization of adversarial images on ImageNet.** I2A generates natural and diverse perturbations based on the text instructions.

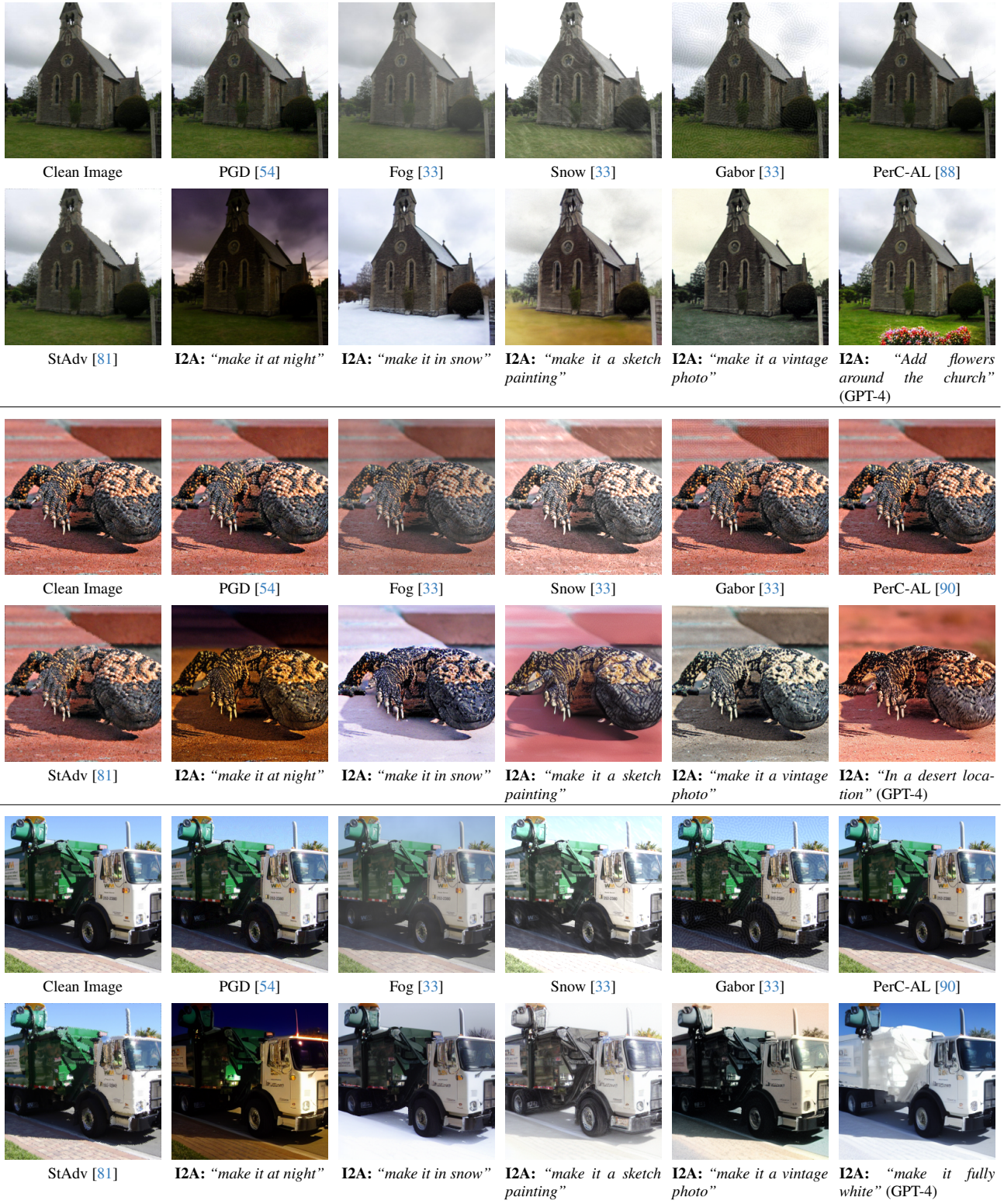


Figure C. Visualization of adversarial images on ImageNet. I2A generates natural and diverse perturbations based on the text instructions.

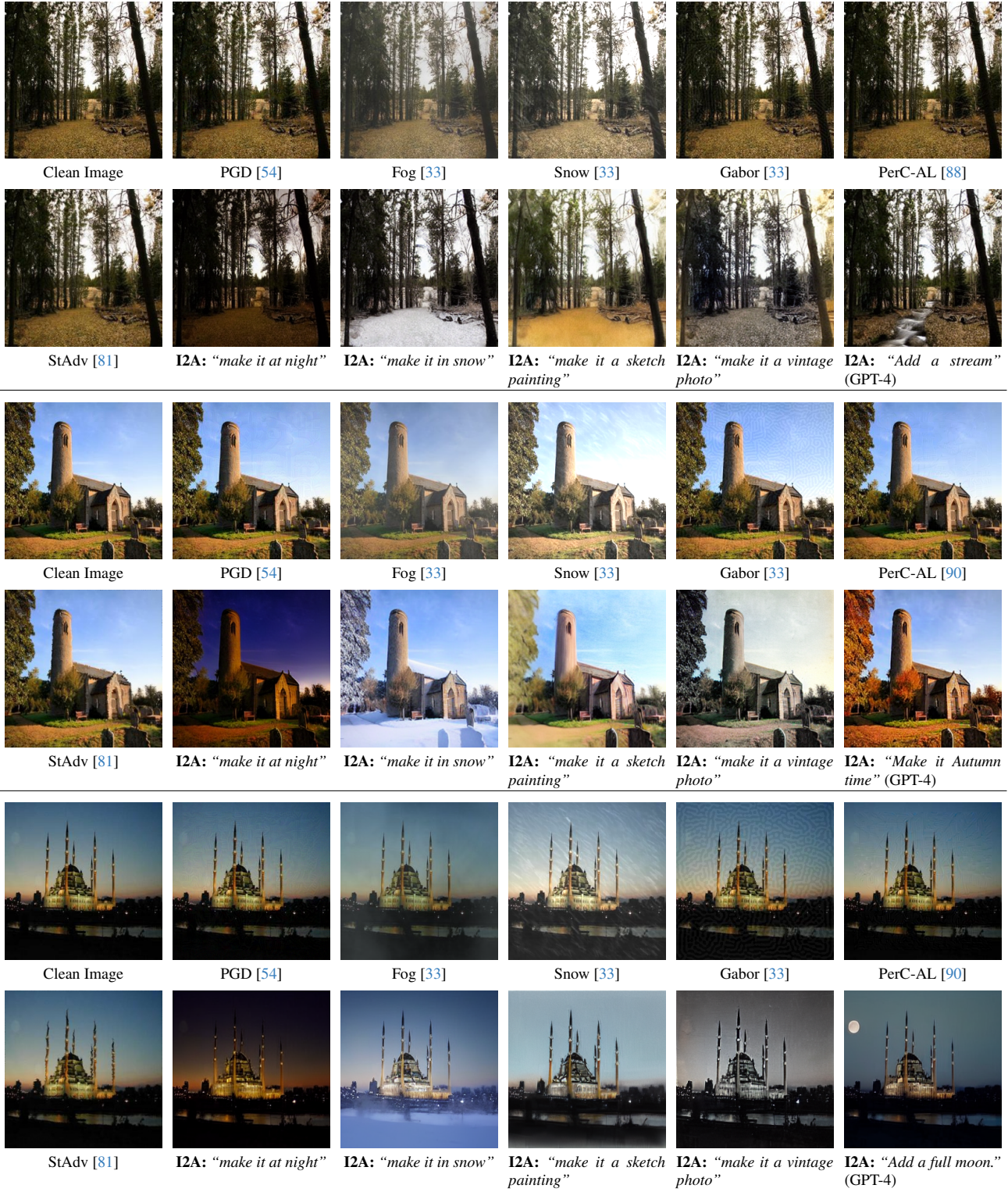


Figure D. **Visualization of adversarial images on Places365.** I2A generates natural and diverse perturbations based on the text instructions.

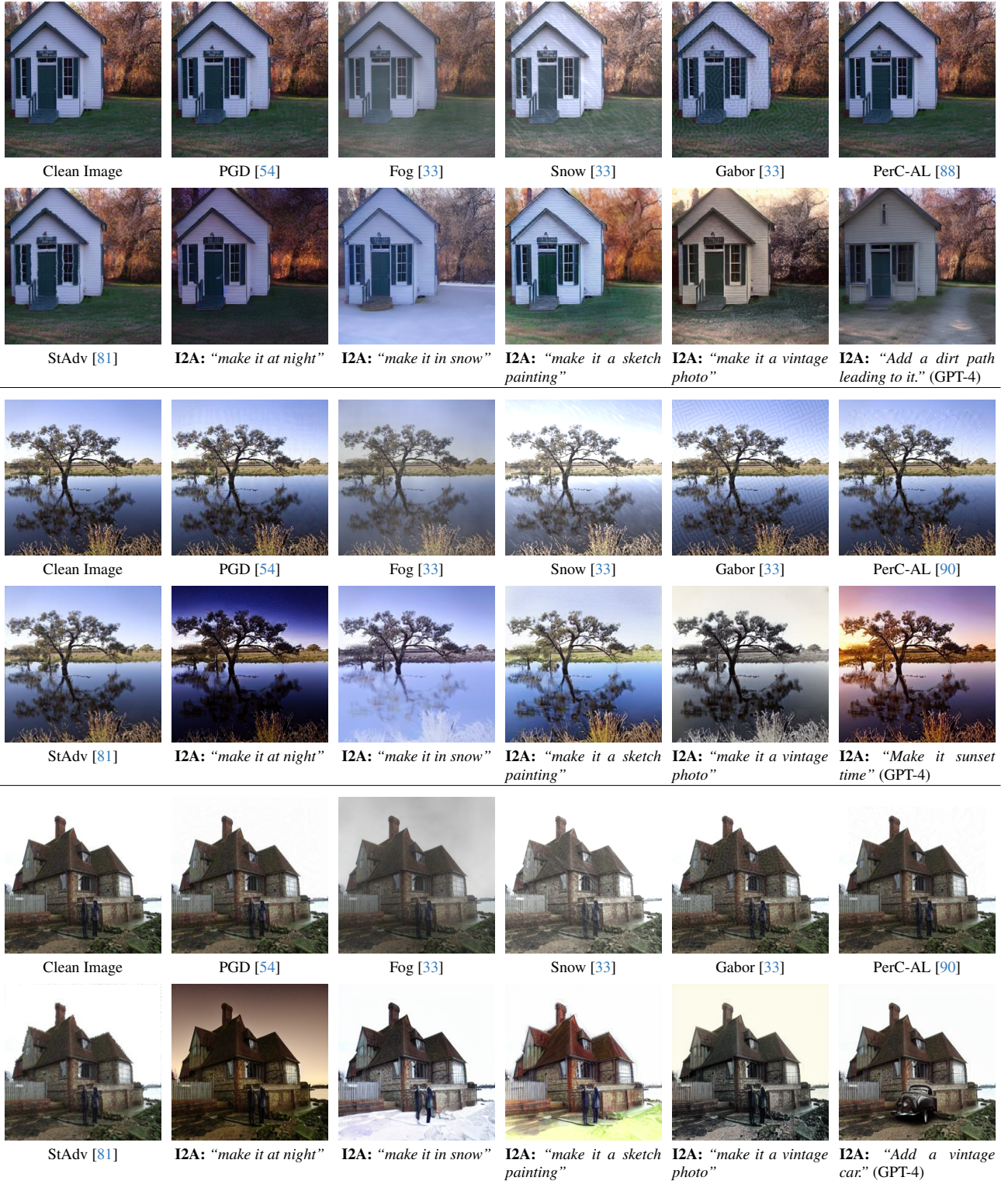


Figure E. **Visualization of adversarial images on Places365.** I2A generates natural and diverse perturbations based on the text instructions.

You are now tasked with generating image editing instructions for an advanced image editing algorithm. When given an image caption, your role is to produce a corresponding image editing instruction without altering the inherent nature or category of objects within the image.

Guidelines:

1. Do not alter the primary category of objects. For instance, if the caption mentions a “beer glass”, avoid instructions that would change it to a “wine glass”.
2. Preserve the natural and typical attributes of objects. Hence, if the caption mentions a “green mamba”, don’t instruct to change its color, given that green mambas are characteristically green.
3. Ensure that the resulting scene remains plausible. For example, if the caption says, “a young orangutan standing on a rock”, refrain from suggesting changes like “make the rock green”, which would create an unnatural scenario.
4. Refrain from introducing drastic global alterations like changing indoor scenes to outdoor.
5. Be aware of potential errors in the captions and adhere to the object “category”.
6. Prioritize Simplicity. Keep the edits straightforward and uncomplicated.

Here are some examples:

{“input”: “a close up of a gun on a soldier’s shoulder”, “edit”: “as if it were a drawing”, “output”: “a drawing of a gun on a soldier’s shoulder”, “category”: “assault rifle”}

{“input”: “a small chinchilla is being fed a toothbrush”, “edit”: “make the chinchilla white”, “output”: “a white chinchilla is being fed by a syringe”, “category”: “syringe”}

{“input”: “a close up of a spider with orange legs”, “edit”: “as a painting”, “output”: “a painting of close up of a cockroach with orange legs”, “category”: “cockroach”}

{“input”: “an old theater curtain with a light shining through it”, “edit”: “turn off the light”, “output”: “an old theater curtain without light shining through it”, “category”: “theater curtain”}

{“input”: “a laptop computer sitting on a desk with a keyboard”, “edit”: “make it black”, “output”: “a black laptop computer sitting on a desk with a keyboard”, “category”: “notebook”}

{“input”: “a dog standing on a dirt road next to a pole”, “edit”: “make it at night”, “output”: “a dog standing on a dirt road next to a pole during the night”, “category”: “malinois”}

{“input”: “a black and white photo of a spiral garden”, “edit”: “make it more colourful”, “output”: “a colourful photo of a spiral garden”, “category”: “maze”}

{“input”: “a close up of a curtain with a pattern on it”, “edit”: “make it blue”, “output”: “a close up of a blue curtain with a pattern on it”, “category”: “shower curtain”}

{“input”: “a large dinosaur statue with a big mouth”, “edit”: “add some snow”, “output”: “a large dinosaur statue with a big mouth in snow”, “category”: “triceratops”}

{“input”: “a bug on the hood of a car”, “edit”: “on Mars”, “output”: “a bug on the hood of a car on Mars”, “category”: “walking stick”}

{“input”: “a woman wearing a black jacket next to a vending machine”, “edit”: “change the jacket to a cape”, “output”: “a woman wearing a black cape next to a vending machine”, “category”: “vending machine”}

{“input”: “a brown and tan pitcher with a handle on a table”, “edit”: “Make it look like an old photograph”, “output”: “an old photograph of a brown and tan pitcher with a handle on a table”, “category”: “pitcher”}

{“input”: “a metal gate with a shadow on it”, “edit”: “as if it was a painting”, “output”: “a painting of a metal gate with a shadow on it”, “category”: “turnstile”}

.....

{“input”: “a green jeep parked in front of a white building”, “edit”: “make the jeep red”, “output”: “a red jeep parked in front of a white building”, “category”: “jeep”}

Please write edits for the following samples:

{“input”: “a river flowing through a valley with snow capped mountains”, “category”: “valley”, “edit”: “”, “output”: “”}

.....

Table E. **Prompt for GPT-4 to generate edit instructions.** We provide 50 manually written examples and ask GPT-4 to generate the edits for the other images given the image captions and object categories as input.